Calibration of the Virgo gravitational wave detector: exploring the contribution of phase information

SOREL Thibault
M2 Internship defence
Supervised by Pierre Van Hove

Strasbourg University

18/06/2026

Gravitational waves and CBC scenario

- Gravitational waves are generated by accelerating masses and deformed space-time metrics during their propagation :

$$g_{\mu\nu} = \eta_{\mu\nu} + h_{\mu\nu} \tag{1}$$

- Generated by compact binary coalescence, such as two neutron stars or two black holes.
- Follows a characteristic scenario : energy emission, increases in rotation speed and the merger of the two objects.

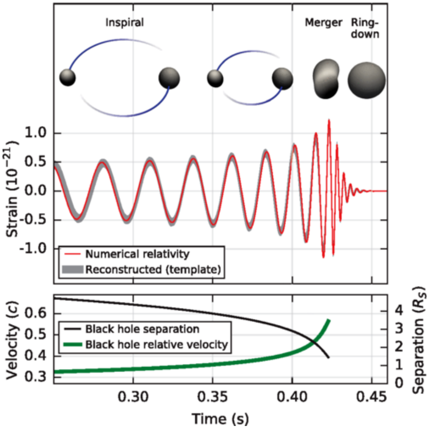

Figure 1 : GW150914 event scenario

Interferometer principle and Virgo experiment

- Interferometer principle : LIGO, Virgo and Kagra.

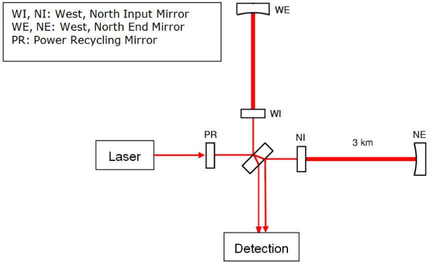

Figure 2 : Simplified Virgo optical scheme

- Relation between strain and deformation

$$h = \frac{\Delta L}{L}$$

- The output signal of the interferometer is a voltage.
- Goal of calibration : establish a law between deformation (ΔL) and measured signal (Volt).

Calibration at Virgo and few systems

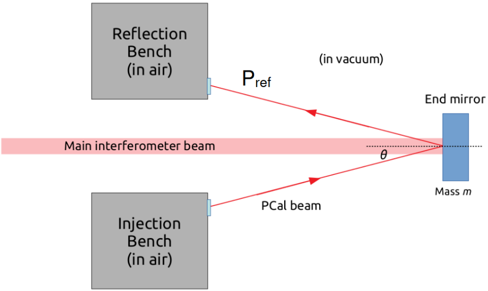

Figure 3 : Scheme of PCal behavior

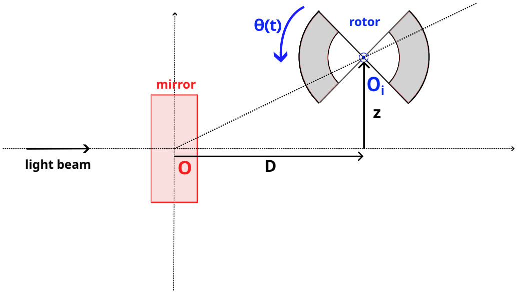

Figure 4 : Newtonian calibrator picture at IPHC

Newtonian calibration (NCal)

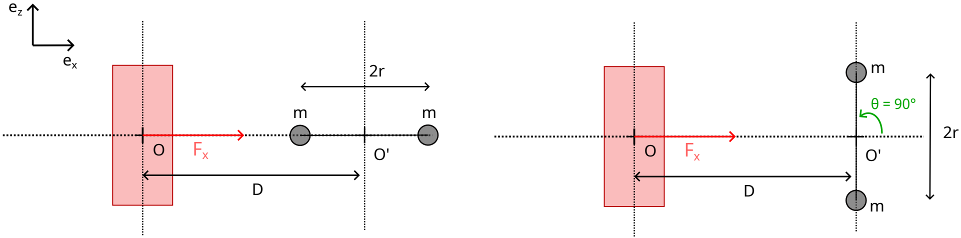

Figure 5 : Two point masses example

- Two characteristic positions : maximal force when aligned, minimal force when perpendicular.
- Rotor rotation modulates the gravitational force applied to the mirror.

$$F_x = C\ cos(2\theta(t))$$

Real geometry of NCal

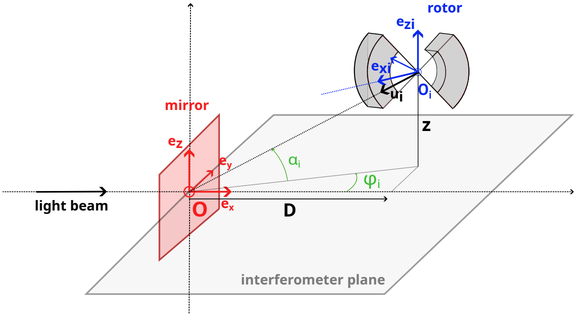

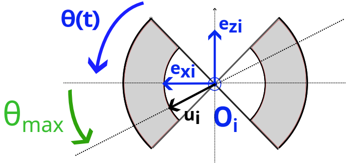

$$F_x(t) = C\cos(2\theta(t) + \phi)$$
$$\phi \approx -\frac{8}{3}\frac{z}{d}$$

Figure 6 : Rotor and mirror geometrical system with associated rotor frame and West Building rotors.

Rotor position in the West End Building (WEB)

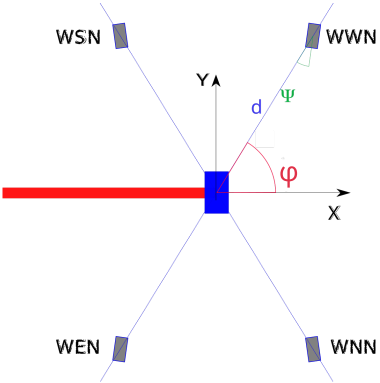

Figure 7 : Four rotors in the West End Building (WEB)

- Motivation :
  Analyse the phase of the output signal and extract geometrical information
- Finally, obtain mirror-rotors relative vertical position

Finite elements analysis

- FROMAGE software

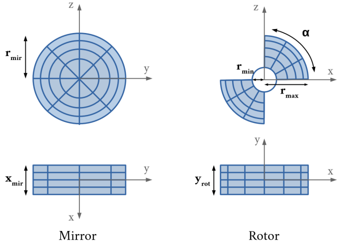

Figure 8 : Mirror and rotor geometry discretisation.

Force computation

$$\vec{F}_{A/B} = G \sum_A \sum_B \frac{m_A m_B}{d_{A,B}^2} \vec{u}_{AB}$$

Simulation with FROMAGE to determine laws

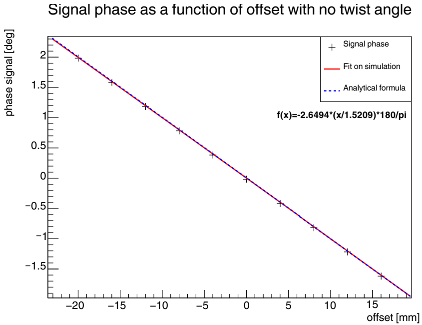

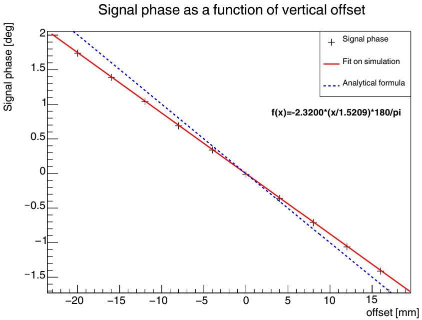

No twist angle : analytical slope close to $-8/3 = -2.66$.

Nominal twist angle : fitted slope -2.32.

$$z(\phi_{2\nu}) = d\,\frac{\phi_{2\nu}}{-2.32} \implies \sigma_z = \left|\frac{d}{-2.32}\right| \sigma_\phi$$

Two-month analysis : injected frequency lines

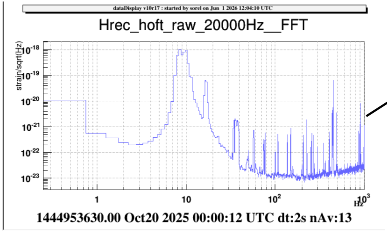

FFT spectrum of measured strain

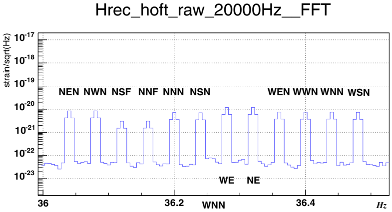

Frequency lines injected by NCals and PCals in the measured strain spectrum.

Line identification

Source	Frequency lines [Hz]
NEB rotors	36.04, 36.08, 36.12, 36.16, 36.20, 36.24
PCal lines	36.28, 36.32
WEB rotors	36.36, 36.40, 36.44, 36.48

Two-month analysis : stable data selection

Locking step (yellow areas = ITF not locked)

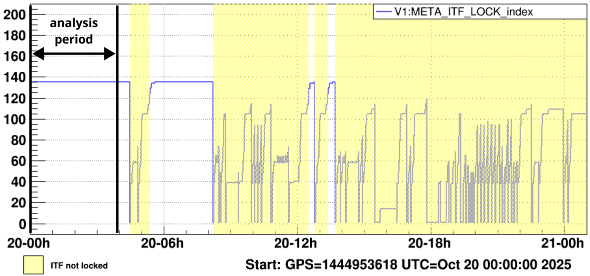

Interferometer lock status on 20 Oct. 2025. White regions are selected for phase analysis.

- 2 month analysis was performed.
- Criteria were verified : locked interferometer, stability in frequency.

Analysis in time of all rotor phases

- FFT analysis and phase extraction at the rotor frequency

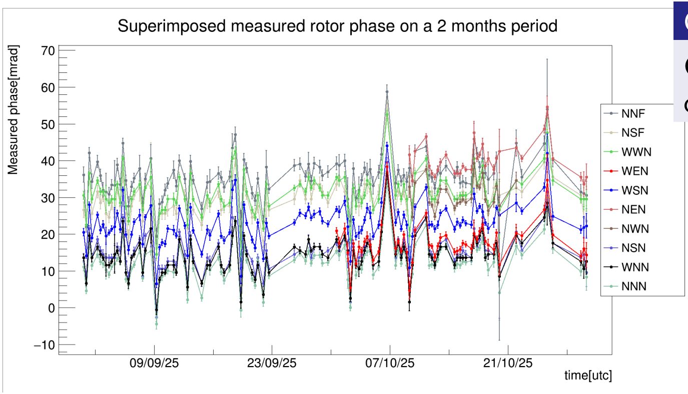

Observation

Common tendency, i.e. correlated variations.

- Retrieve a stable rotor phase for everyone and compare.
- NSN is chosen as a stable rotor.

- Possibility to attenuate variation : subtract the NSN line to everyone.

Phase stability after NSN subtraction

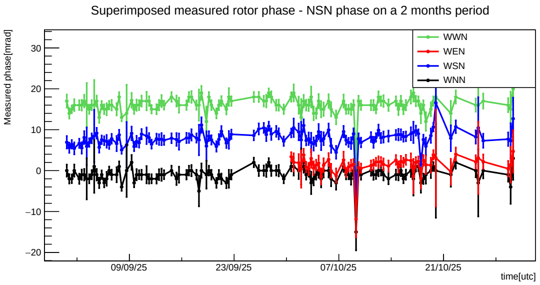

Figure 9 : Rotor phases after subtraction of NSN.

Rotors	σ_ϕ (mrad)	$\sigma_{\phi_{NSN}}$ (mrad)
WNN	5.3	1.9
WEN	5.4	2.3
WSN	5.4	2.2
WWN	5.4	1.9
NNF	6.2	2.8
NSF	5.5	2.3
NEN	4.5	2.4
NWN	3.8	1.8
NSN	5.4	0.0
NNN	5.3	1.3

Table 1 : Standard deviation of phase distribution without and with subtraction of NSN rotor phase.

Method to extract geometrical information from signal phase

- Phase difference gives :

$$\theta_{\text{max}}$$

- Common acquisition phase cancels :

$$\phi_{\mathrm{acq}}$$

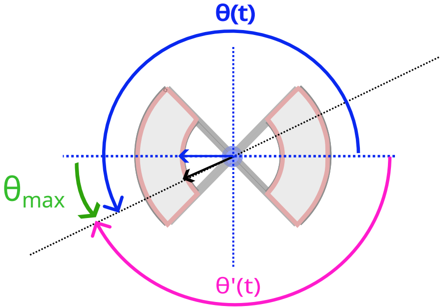

Figure 10 : Scheme of link between rotation phase and geometrical angle

Choice of the two analysis periods and criteria

Selected analysis periods

Period 1	**Period 2**
20 Oct. 2025, 00 :00 UTC	22 Nov. 2025, 14 :00 UTC
$t_1 = 1444953618$	$t_2 = 1447855218$

Opposite rotation directions $\Rightarrow$ extraction of θ_{max}, then estimation of Δz.

Rotors	**20th Oct.**	**22th Nov.**
WNN	up	down
WEN	up	down
WSN	up	down
WWN	down	up

Table 2 : Synthesis of west rotors disposition during analysis time obtained from Virgo logbook history

Results and vertical offset determination

For each west building rotor, the measured phase is used to extract $\theta_{\max}$ and deduce the relative vertical offset z.

Rotors	$\boldsymbol{\phi = \theta_{\max}}$ (mrad)	$\boldsymbol{\Delta\phi}$ (mrad)	$\boldsymbol{z}$ (mm)	$\boldsymbol{\Delta z}$ (mm)
WNN	-6.70	0.44	4.39	0.29
WEN	-12.22	0.46	8.01	0.30
WSN	-7.00	0.44	4.59	0.29
WWN	-1.91	0.46	1.25	0.30

Table 3 : Mean phase and corresponding estimated relative position for each west building rotors

Geometrical measures of rotors in the VRF (Virgo Reference Frame)

The survey group measures the vertical position of each West Building rotor, used as a geometrical reference for the mirror position estimation.

Coordinates	$\boldsymbol{X}(m)$	$\boldsymbol{Y}(m)$	$\boldsymbol{Z}(m)$
BS	0.0027	0.0232	-0.0030
NE	0.0129	3005.7877	-0.9020
WE	-3005.5847	0.0312	-2.2233

Table 4 : Coordinates in Virgo frame of the Beam Splitter, North End mirror and West End Mirror.

Rotor	$\boldsymbol{Z_r}$ (m)	$\boldsymbol{\sigma_Z}$ (mm)	$\boldsymbol{Z_r - Z_m}$ (mm)
WNN	-2.2181	0.9	4.3
WEN	-2.2144	0.8	8.9
WSN	-2.2193	0.7	4.0
WWN	-2.2207	0.3	2.6

Table 5 : Vertical coordinates in Virgo frame of West Building rotors, uncertainty on geometrical measurement and relative position to the estimated mirror center.

Results of mirror position estimation

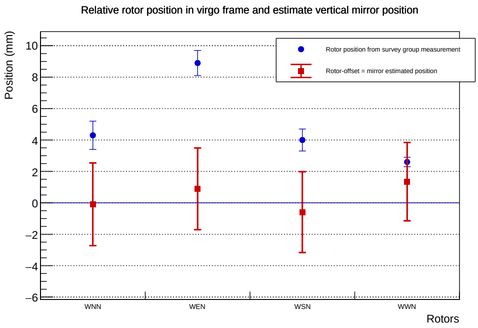

Figure 11 : Mirror position from geometrical survey and phase estimation.

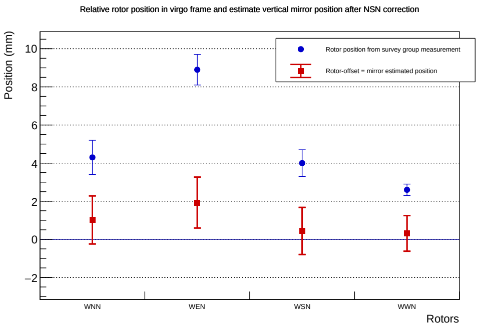

Figure 12 : Mirror position after NSN phase correction.

Improvement of signal uncertainties

Injected motion amplitude :

$$a(\nu) = \frac{C}{M\left(2\pi(2\nu)\right)^2}$$

This analysis

Worst-case from measured positions

$$\frac{C_{\max}}{C_{\min}} = 1.000043$$

$$\Delta_{\text{offset}} = 0.0043\%$$

Conclusion

- Phase information gives access to the rotor–mirror vertical offset.
- The measured phases are stable over time and agree with geometrical measurements.
- The uncertainty from the vertical offset remains small compared with the projected rotor–mirror distance uncertainty.

Thanks for your attention !

West building rotors phases normalized by NSN phase

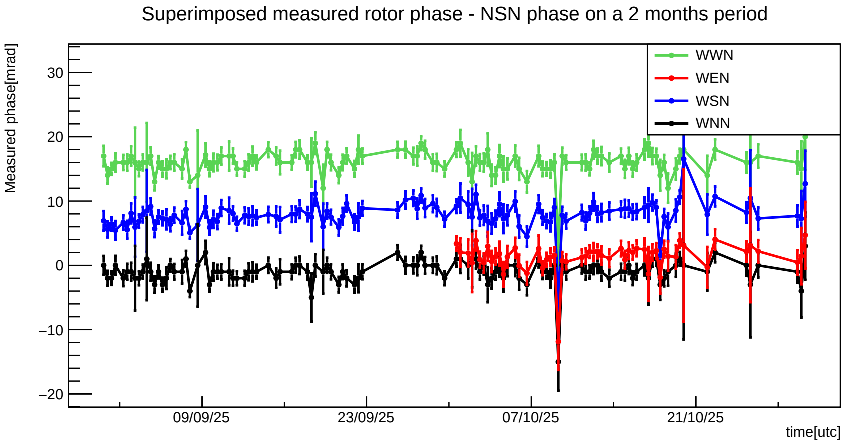

West rotors phase for two months after subtracting NSN phase.

Phases of WEB rotors and NE PCal

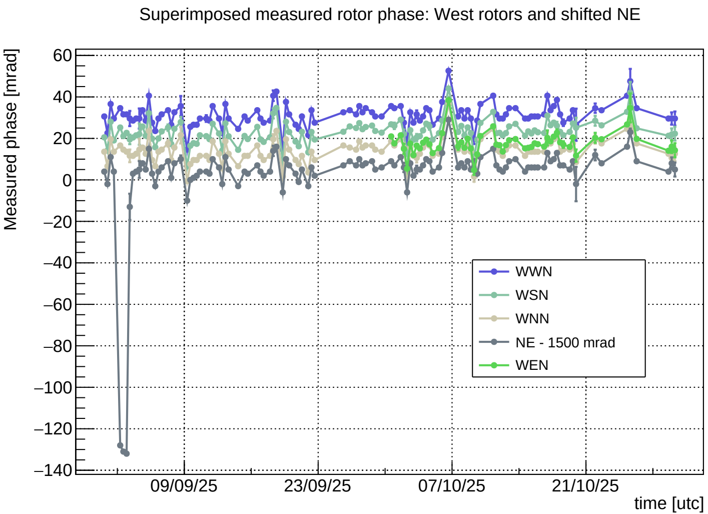

Convergence of FROMAGE computation

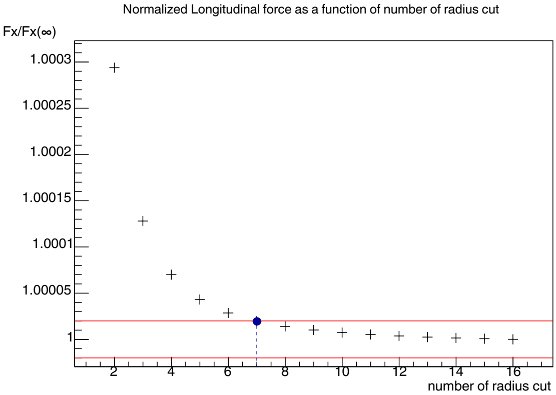

Numerical longitudinal force convergence with radius cuts.

Modulated force term and relations

$$F_x(t) = C\cos(2\theta(t) + \phi)$$

$$C \quad \Longrightarrow \quad C = \frac{9G}{8D^4}\,\rho_{\mathrm{rot}}\, b\left(r_{\mathsf{max}}^4 - r_{\mathsf{min}}^4\right)\sin(\alpha)\,\rho_{\mathrm{mir}}\,\pi r_{\mathrm{mir}}^2 x_{\mathrm{mir}}\, \cos(\Phi)\left(A^2 + B^2\right)^{1/2}$$

$$\phi \quad \Longrightarrow \quad \phi \approx -\frac{8}{3}\frac{z}{D}$$